Journal of Applied Polymer Science

Facile Synthesis of Amphiphilic Chitosan-*g*-Poly(lactic acid) Derivatives and the Study of Their Controlled Drug Release

Hong-Wei Lu,[1] Hong He,[1] Bin Zhang,[2] Guo-Qiang Liu,[1] Meng-Yao Li,[1] Qiu-Lin Nie[1]
[1]College of Materials & Environmental Engineering, Hangzhou Dianzi University, Hangzhou 310018, China
[2]School of Physics and Electronic Engineering, Jiangsu Normal University, Xuzhou 221116, China
Correspondence to: H.-W. Lu (E-mail: luhongwei@hdu.edu.cn)

ABSTRACT: We report here a simple and green procedure for the synthesis of amphiphilic chitosan (CS) derivatives with poly(lactic acid) (PLA) side chains, without the use of high pure lactide, high temperatures, or large amounts of organic solvent. The chemical structure and physical properties of these CS derivatives were characterized by Fourier transform infrared spectroscopy, ^{1}H-NMR, thermogravimetric analysis, and X-ray diffraction. The formation and characteristics of polymeric micelles based on these CS derivatives were studied by fluorescence spectroscopy and dynamic light scattering. The critical aggregation concentration in water varied from 0.048 to 0.021 mg/mL, and the mean diameter was in the range 169.8–260.7 nm in aqueous solution at 25°C when the PLA grafting percentage increased from 92 to 132%. Transmission electron microscopy showed that the micelles exhibited a nanospheric morphology within a size range of 60–120 nm. For the resulting micellar aggregates, the drug loading and *in vitro* drug-release characteristics were studied with indomethacin as the model drug. We found that such micellar aggregates could be potentially used as nanocarriers for drug delivery. © 2013 Wiley Periodicals, Inc. J. Appl. Polym. Sci. 130: 908–915, 2013

KEYWORDS: biomedical applications; functionalization of polymers; polyesters; polysaccharides; self-assembly

Received 12 October 2012; accepted 18 February 2013; published online 11 April 2013
DOI: 10.1002/app.39205

INTRODUCTION

Chitosan (CS) is an amine-rich polysaccharide derived by the deacetylation of chitin. Chitin is the second most abundant polysaccharide in nature; it is found in crustaceans, insects, and fungi.[1] There has been increasing interest in the exploration of potential uses for CS in the development of new functional biomaterials for applications in various fields.[2–5] Because of its high crystallinity and strong intermolecular and intramolecular hydrogen bonding between polymer chains, CS is only soluble in dilute acidic solutions and special halogen-containing organic solvents.[6] Furthermore, the polyelectrolyte solutions formed by CS have limited applications as transition metal sorbents and drug carriers because bioactive agents may be affected by acetic acid. Since the 1950s, although considerable efforts have been made to chemically modify CS to impart specific properties and distinctive biological functions, including solubility,[7,8] it remains a challenge to develop a new processing strategy to broaden the potential applications of this biorenewable resource.[9]

Poly(lactic acid) (PLA), a poly(2-hydroxypropionic acid), is one of the most well-known and extensively studied polymers prepared from biorenewable feedstock.[10] To minimize the adverse impact of chemicals on our environment and to find alternatives to replace depleting petrochemical resources, PLA has been found to be an ideal candidate for polymeric commodities (e.g., packaging materials for food and beverages, plastic bags, thin film coatings) and biomaterials (e.g., for medical devices, sutures, tissue replacements, delivery vehicles).[11] So far, most graft copolymers of CS and PLA have been prepared via the ring-opening polymerization of lactide with high purity or the end-group coupling of PLA with reactivity. However, both approaches involve lactide with a high purity, large amounts of energy, and an organic solvent. The ring-opening polymerization (ROP) of lactic acid *in situ* with $Sn(Oct)_2$ as a catalyst and hydroxyls on glucose rings as an initiator, which has been proven to be an effective method for synthesizing polysaccharide/polyester composites, would be a green method for preparing CS-*g*-polylactide.

Lactic acid is generally obtained by the fermentation of common sugars rather than petroleum raw materials and is especially practical because of its excellent biocompatibility and biodegradability.[12] In previous studies, we found that CS could be dissolved in lactic acid under moderate conditions. Moreover, lactic acid could generate lactide *in situ* under moderate conditions.[13] In this study, we dissolved CS in lactic acid and then

Table I. Effect of the Feed Ratio and Catalyst Content on GP

Sample	LA (g)	CS (g)	Temperature (°C)	Time (h)	Catalyst content (%)	GP (%)
CS-PLA_{1a}	10	1	120	5	0.1	92.49
CS-PLA_{2a}	20	1	120	5	0.1	101.82
CS-PLA_{3a}	30	1	120	5	0.1	131.72
CS-PLA_{4a}	40	1	120	5	0.1	152.60
CS-PLA_{5a}	50	1	120	5	0.1	167.32
CS-PLA_{1b}	30	1	120	5	0.15	164.02
CS-PLA_{2b}	30	1	120	5	0.20	219.1
CS-PLA_{3b}	30	1	120	5	0.25	242.67
CS-PLA_{4b}	30	1	120	5	0.30	313.42

Pressure = 100 Pa.

directly copolymerized it and lactide *in situ* under moderate conditions. Then, amphiphilic CS derivatives containing side chains of PLA were obtained. Here, lactic acid acted as a green solvent and a starting material, so this new method was proven to be efficient, atomic, economical, and environmentally friendly. The self-assembly of the copolymers to the micelles in an aqueous solution, which showed great potential for the copolymers as a new drug-delivery system, was also demonstrated.

EXPERIMENTAL

Chemicals and Reagents

CS (deacetylation $\geq$ 90%, weight-average molecular weight = 190–375 KDa) was purchased from Shanghai Bio Science & Technology. Co., Ltd. (Shanghai, China). Lactic acid (90% aqueous solution) was purchased from Guanghua Chemical Co. (Guangdong, China). Tin octoate [stannous 2-ethylhexanoate; $Sn(Oct)_2$] was purchased from Alfa Aesar (USA) and was used as received. Pyrene and indomethacin (IND) were purchased from Fluka (USA). Pyrene was purified by two recrystallizations from ethanol and *in vacuo* drying. Dimethyl sulfoxide was dried over molecular sieves and then vacuum-distilled. All other chemicals were analytical grade and were used as received.

Modification Reaction of CS and Characterization

CS (1 g, powder) and lactic acid (10, 20, 30, 40, and 50 g) were added to a 250-mL, three-necked flask equipped with a mechanical stirrer and a vacuum pump system. After it was stirred at 75°C for 30 min, the reaction system was heated to 100°C with a temperature-controlling system. After the CS was fully dissolved in the lactic acid, $Sn(Oct)_2$ (0.1, 0.15, 0.20, 0.25, and 0.3%) was added to the flask. The modification reaction was conducted at 100°C *in vacuo* (100 Pa) for 5 h. After the reaction, the flask was cooled to room temperature. The crude product was washed twice with acetone under vigorous stirring, and then, the final product was dried at 60°C *in vacuo*. The detailed synthetic conditions for the modification in this study are listed in Table I. The grafting percentage (GP) was determined according to the following equation:

$$GP = \frac{(w_2 - w_1) \times 100}{w_1} \quad (1)$$

where w_1 and w_2 are the weights of the CS before and after the grafting reaction, respectively.

The copolymers were characterized by Fourier transform infrared (FTIR) spectrometry (Nicolet 670, USA). ^{1}H-NMR spectra were obtained on a Bruker AV400 spectrometer (Bruker, Germany) at 400 MHz. The graft copolymer was dissolved in D_2O, and its concentration was about 5 mg/mL.

Formation and Characterization of the Micellar Aggregates

The micellar aggregates of the modified CS were prepared by a dialysis method. The modified CS sample (0.5 g, powder) was dissolved in dimethyl sulfoxide. The resulting solution was dialyzed with a dialysis membrane bag with a molecular weight cutoff of 8000 g/mol against deionized water. The deionized water was exchanged every 2 h for the first 6 h and every 6 h for an additional 18 h. Finally, the dialyzed solution was freeze-dried.

The micellar aggregates were examined with a spectrofluorophotometer (RF-5301 PC, Shimadzu, Japan). The excitation wavelength was 330 nm, and the fluorescence emission spectra were recorded from 350 to 500 nm. The morphology of the aggregates was examined with a JEM-2010HR high-resolution transmission electron microscope (Shimadzu, Japan). A drop of sample solution (2 mg/mL) containing 0.2 wt % phosphotungstic acid was deposited onto a 200-mesh copper grid coated with carbon. Excess solution was removed with a Kimwipes delicate wipe. The size and size distribution of the micellar aggregates were examined by dynamic light scattering (DLS) with a BI-200SM goniometer particle size analyzer (Brookhaven, USA). Each analysis lasted for 300 s and was performed at 25°C with a detection angle of 90°. The ζ potentials of the micellar aggregates were measured with a Powereach JS94H microelectrophoresis unit (Shanghai, China).

Drug Loading by Micellar Self-Aggregates

The loading of the hydrophobic IND in the inner cores of the resulting micelles was carried out by a solvent evaporation method. The micelle sample was first dispersed in 70 mL of phosphate buffer solution (pH 7.4), and then, 5 mL of IND–ethanol solution (1 mg/mL) was added slowly to the micelle dispersion under stirring. After that, stirring was continued at 50°C for 24 h in air for the encapsulation of IND in the

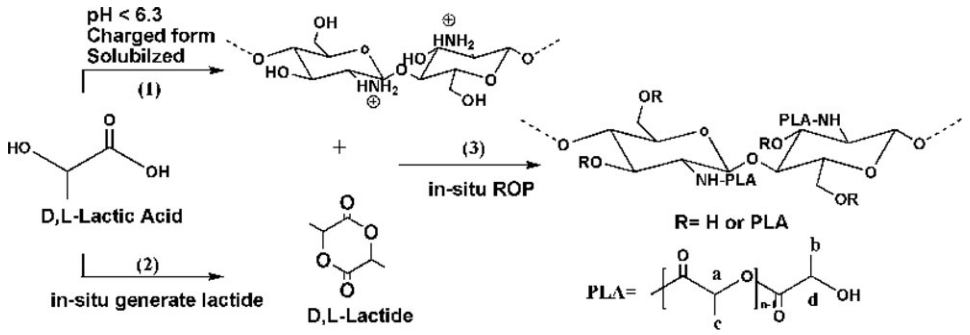

Scheme 1. Synthetic scheme of the amphiphilic CS–PLA.

micellar aggregates and the evaporation of the ethanol. Finally, the system was centrifuged at 4000 rpm for 10 min to remove the unloaded IND, and then, the supernatant with IND-loaded micelles was obtained. The precipitate with unloaded IND was dissolved in a 50% ethanol solution, and its amount was analyzed by UV–vis spectrophotometry (UV-3150, Shimadzu) at 318 nm. The loading capacity (LC) and the loading efficiency (LE) were determined according to the following equations:

$$\mathrm{LC} = \frac{(m_1 - m_2) \times 100}{m_3} \quad (2)$$

$$\mathrm{LE} = \frac{(m_1 - m_2) \times 100}{m_1} \quad (3)$$

where m_1 is the total weight of IND used, m_2 is the weight of unloaded IND, and m_3 is the weight of the micelle sample.

In Vitro Release of the Drug-Loaded Micellar Aggregates

The *in vitro* drug-release study was carried out at 25, 37, and 47°C under magnetic stirring. The lyophilized micellar aggregates loaded with IND were first suspended in a phosphate buffer solution (pH 7.4), then transferred into a dialysis bag with a molecular weight cutoff of 35,000, and subjected to dialysis against 100 mL of distilled water for 24 h (we refreshed the water after 12 h). The volume of solution was held constant by the addition of 2 mL of distilled water after each sampling. The amount of drug released was measured with UV absorbance (UV-3150, Shimadzu) at 318 nm. The cumulative drug release was calculated from the following relationship:

$$\text{Cumulative drug release } (\%) = M_t/M_0 \times 100$$

where M_t is the amount of drug released from the micelles at time t and M_0 is the amount of drug loaded in the polymeric micelles. M_0 was estimated by the subtraction of the amount of unloaded drug from the drug amount in the feed (2.0 mg). The amount of unloaded drug was analyzed by measurement of the absorbance at 242 nm of dialyzate after drug loading.

RESULTS AND DISCUSSION

Characterizations of the Amphiphilic CS Derivatives (CS–PLA)

Teramoto and Nishio[14] studied the *in situ* ROP reaction of cellulose diacetate and a lactic acid solution under the catalyst stannous octoate; their study suggested that the *in situ* ring-opening graft polymerization reaction occurred at the active center where the Sn—O was generated by the reaction between the amino or hydroxyl of CS and stannous octoate.[15] Then, a coordination–insertion mechanism was involved in the ring-opening graft polymerization of lactide generated in the dehydration of lactic acid. Then, amphiphilic CS derivatives containing side chains of PLA were obtained as shown in Scheme 1.

Table I shows the effect of the feed ratio and catalyst content on GP. When the catalyst content was fixed at 0.10%, GP became larger with increasing lactic acid content. When the mass ratio of lactic acid to CS increased from 10 : 1 to 50 : 1, GP also increased from 92.49 to 167.32%. Therefore, when the catalyst concentration was fixed, GP increased with increasing lactic acid content; this was consistent with the results of other studies on ring-opening graft polymerization with triethylamine as a catalyst.[16] Moreover, when the mass ratio of lactic acid to CS was fixed at 30 : 1 with the stannous octoate catalyst content increasing from 0.10 to 0.30%, GP increased from 131.72 to 313.42%. This was attributed to the oxygen in the synthetic process, which may have consumed part of the stannous octoate and resulted in the partial inactivation of the catalyst.

Figure 1 shows the FTIR spectra of CS and CS–PLA_{1a}. In the spectra of CS, there was a multiple absorption peak at 3400 cm^{-1} formed by the overlap of stretching vibration peaks with the broad peak of O—H and N—H.[17] The 2853- and 2923-cm^{-1}

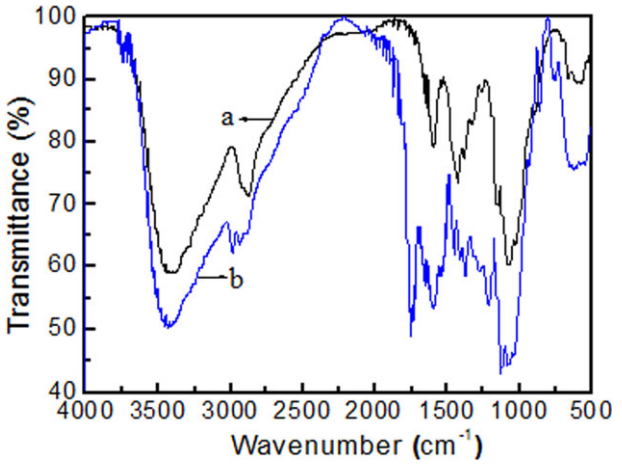

Figure 1. FTIR spectra of (a) CS and (b) CS–PLA_{1a}. [Color figure can be viewed in the online issue, which is available at wileyonlinelibrary.com.]

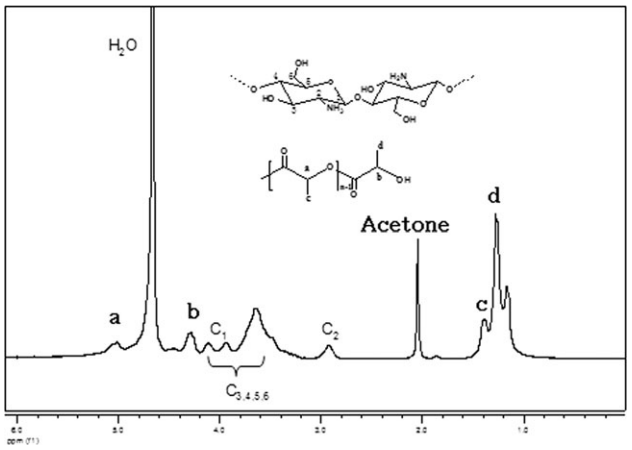

Figure 2. ^{1}H-NMR spectrum of CS–PLA$_{1a}$ in D_2O. The molecular structure shows inset accordingly. a and b and c and d in the molecular structure and ^{1}H-NMR spectrum represent protons in —CH and —CH_3 in PLA, respectively.

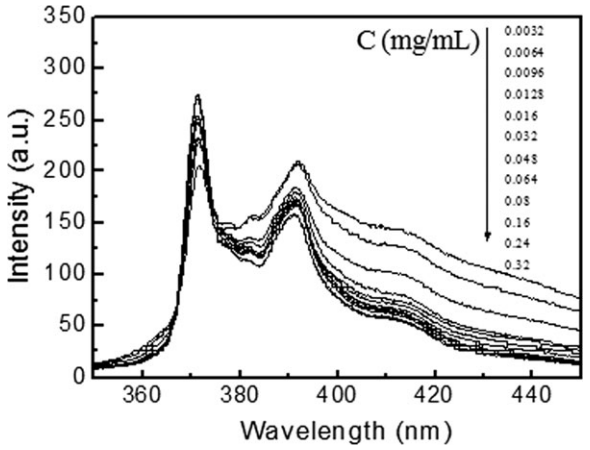

Figure 3. Effect of the polymer concentration (C) on the fluorescence emission spectra of pyrene in water in the presence of CS–PLA$_{2a}$.

doublets observed in CS were assigned to C—H stretching vibration peaks of methyl and methylene on the rings of CS. The peak at 1531–1637 cm^{-1} was a broad mixed absorption band formed by the deformation vibration peaks of CS acid amides I (C—O), acid amides II (N—H), and —NH_2. Compared with the IR spectra of CS (peak a), the broad peak at 3400 cm^{-1} of the spectra of CS–PLA$_{1a}$ (peak b) did not change significantly before and after the reaction. The enhancement of the C—H stretching vibration peak at the 2853- and 2923-cm^{-1} doublets implied the introduction of —CH_3- and —CH_2-containing alkyl substituents in the CS molecules; the new sharp peak at 1750 cm^{-1} was assigned to carbonyl moiety absorption and indicated the successful grafting of the PLA side chain to the backbone of CS.

From the ^{1}H-NMR spectrum of CS–PLA$_{1a}$ in D_2O, shown in Figure 2, we observed that 1.85 ppm referred to the proton peak of acetyl on CS; 2.95 ppm was the proton peak of C-2 on CS. The multipeak at 3.3–3.7 ppm was the proton peak of C-3, C-4, C-5, and C-6 on CS; 3.94–4.18 ppm was the proton peak of C-1 on CS, which conformed to the ^{1}H-NMR spectrum of CS as a reference. The proton peaks at 4.28 ppm (peak b), 5.06 ppm (peak a), 1.23 ppm (peak d), and 1.34 ppm (peak c) were attributed to the proton peaks of methylene and methyl in PLA. Both the FTIR spectra in Figure 1 and the ^{1}H-NMR spectrum in Figure 2 proved that PLA was successfully grafted onto the backbone of CS.

The X-ray diffraction patterns (not shown) of CS–PLA showed typical features of α-CS, with the 2θ of 11.8° disappearing; this indicated that the intramolecular and intermolecular hydrogen bonding in CS was significantly weakened after PLA grafting; this was consistent with previous reports.[18,19] On the basis of thermogravimetric analysis measurements, the thermal degradation of the graft copolymers involved two processes: the thermal degradation of the PLA moiety first, followed by the thermal degradation of the CS backbone. As shown in Table II with increasing GP, the PLA content of the derivatives gradually increased, and the 50% weight loss temperature decreased from the original 364.3 to 247.1°C. The residual quality also decreased correspondingly from 35.6 to 10.4%. These results indicate that the PLA side chains effectively broke the highly crystalline region formed by the hydrogen-bond networks of CS and then made the tough CS less thermally stable.

Micelle Formation and Characterization

It is well known that amphiphilic copolymers with a suitable hydrophilic/hydrophobic balance can form a micellar structure when exposed to a selective solvent. The amphiphilic nature of the CS–polylactide graft copolymers, consisting of hydrophilic CS and hydrophobic polylactide segments, provided an opportunity for the formation of micelles in water. The micelle behavior of CS–PLA in aqueous media was monitored by fluorometry in the presence of pyrene as a fluorescence probe.[20,21] Figure 3 shows the fluorescence emission spectra of the pyrene incorporated into the CS–polylactide polymeric micelles (CS–PLA$_{2a}$) in water at 25°C. If micelles or other hydrophobic microdomains are formed in an aqueous solution, the pyrene preferably lies

Table II. Chemical Compositions and Properties of the Amphiphilic CS Derivative Micelles

Sample	GP (%)	T_h (°C)	Char yield (wt %)	CAC (mg/mL)	D_H (nm)	PDI	ζ potential (mv)
CS	—	364.3	35.6%	—	—	—	—
CS-PLA$_{1a}$	92.49	300.7	22.4%	0.048	169.8	0.362	+30.5
CS-PLA$_{2a}$	101.82	287.1	14.7%	0.036	207.2	0.101	+28.7
CS-PLA$_{3a}$	131.72	247.1	10.4%	0.021	260.7	0.083	+25.1

T_h is the 50% weight loss temperature, PDI is the polydispersity.

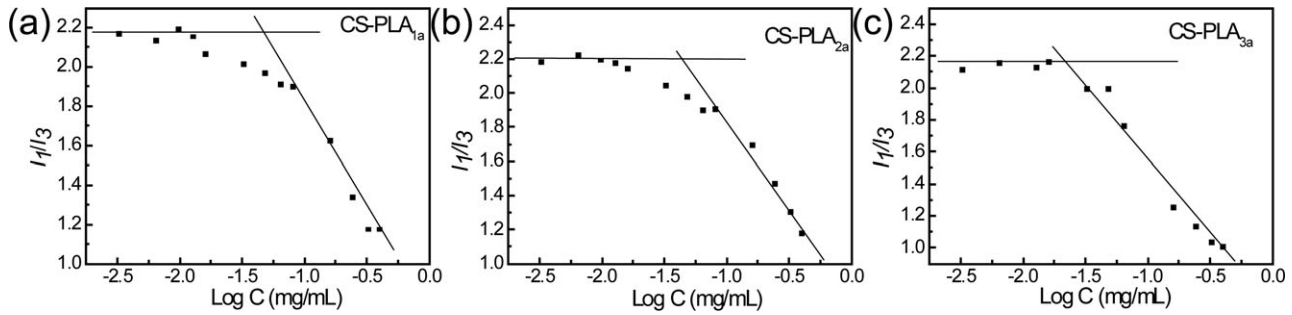

Figure 4. Changes in the intensity ratio (I_1/I_3) versus the concentration (C) of the amphiphilic CS derivatives: (a) CS–PLA_{1a}, (b) CS–PLA_{2a}, and (c) CS–PLA_{3a}.

close to (or inside) these microenvironment and strongly emits when it is quenched in polar media. When the pyrene coexists with polymeric micelles, the total emission intensity increases, and particularly, the intensity of the third highest vibrational band at 383 nm (I_3) starts to drastically increase at a certain concentration of polymeric amphiphiles. In the study of the formation of micelles from a hydrophobically modified graft copolymer in an aqueous solution, pyrene is generally used as a molecular probe, and the variation in the ratio of intensity of the first vibronic peaks I_1 (372 nm) to third (383 nm) vibronic peaks (I_1/I_3), the so-called polarity parameter, is quite sensitive to the polarity of the microenvironment where pyrene is located. Thus, the change in I_1/I_3 can characterize the formation of micelles. Figure 4 shows the changes in the intensity ratio (I_1/I_3) versus the concentrations of the amphiphilic CS derivatives. The inflection point of the two straight lines was the critical aggregation concentration (CAC) of the amphiphilic derivatives. The CAC values of different derivatives are listed in Table II. As shown, with increasing GP from 92.49 to 131.72%, CAC decreased from 0.048 to 0.021 mg/mL. The CAC values of the amphiphilic CS derivatives synthesized in this study were similar to the CAC values of CS derivative micelles reported in the references.[23,24] The hydrophobicity of PLA caused the aggregation of molecular chains to form micelles, so the introduction of a large amount of hydrophobic groups may have reduced the critical micelle concentration values.

As for amphiphilic derivatives, nonpolar interaction among hydrophobic groups and the flexibility of molecular chains in the main chain will affect the volume of micelles.[25] Single-molecule micelles with a relatively small volume are hard to form because of the rigid nature of CS. Instead, micelles with a relatively large volume dependent on intermolecular hydrophobic interactions dominate here. The size of the polymeric micelles and their size distribution in aqueous media were measured by DLS. Because the unmodified CS did not form micelles, it could not be used as a control. Particle size distribution histograms of the CS–PLA micelles determined by DLS are shown in Figure 5. Figure 5(a–c) shows the particle size distributions of the CS–PLA micelles with three different GPs. The obtained D_H (Hyrodynamic diameter) and polydispersity values are listed in Table II. It can be seen from the table II that with increasing GP, the size of the micelles gradually increased. As GP increased from 92.49 to 131.72%, the micelles size increased from 169.8 to 260.7 nm, whereas the polydispersity of the micelles gradually decreased. The ζ potential of the CS–PLA micelles were measured with a Powereach ζ potential measuring instrument (JS94H, Shanghai, China). The CS–PLA micelles exhibited a positive charge ζ potential at 25.1–30.5 mV; this suggested that the PLA was packed in the nanoparticles because its ζ potential was −35.2 mV.

The morphology of the polymeric micelles was investigated by the transmission electron microscopy technique. Figure 6 shows the transmission electron microscopy (TEM) image of the polymeric micelles (CS–PLA_{1a}). We confirmed that the polymeric micelles were spherical in shape. A similar morphology was also observed in the other polymeric micelles of CS–PLA with different molar ratios (data not shown). The size of these micelles was smaller than that determined by DLS in water; this presumably arose from the dry state of the TEM measurement.

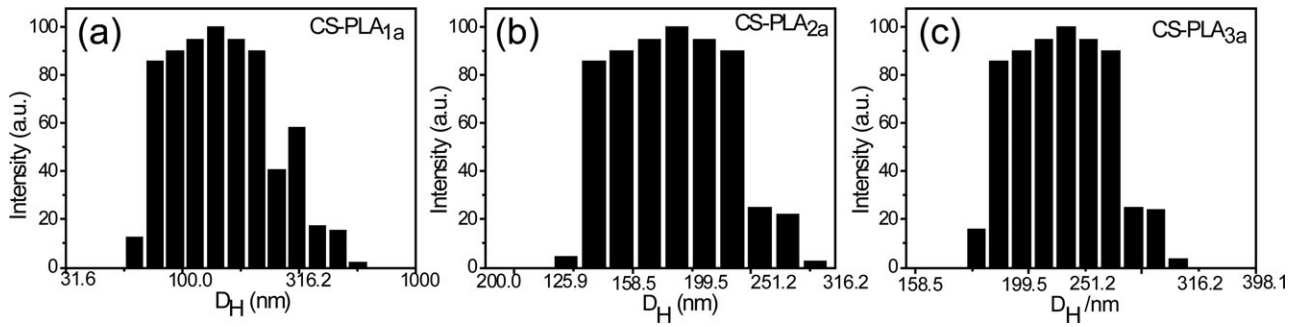

Figure 5. Particle size distributions of the amphiphilic CS derivative micelles determined by DLS: (a) CS–PLA_{1a}, (b) CS–PLA_{2a}, and (c) CS–PLA_{3a}.

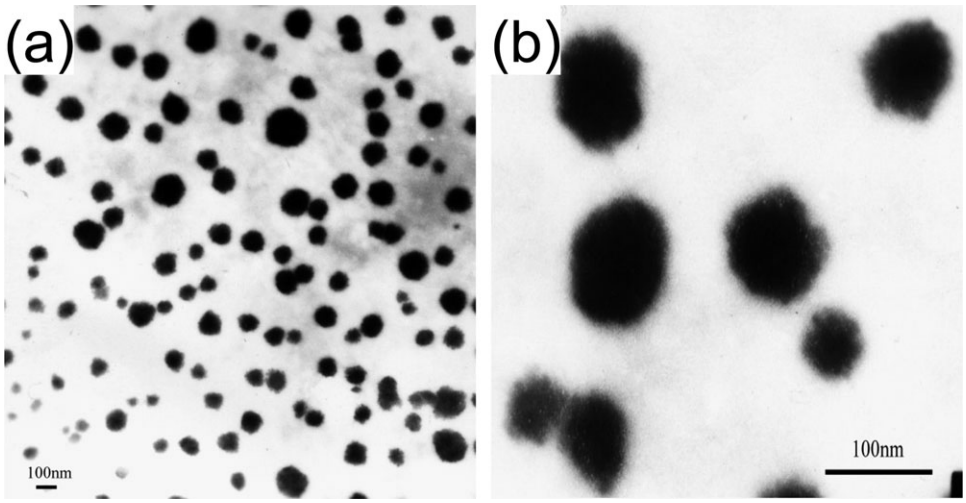

Figure 6. TEM micrographs of the CS–PLA_{1a} micelles. The scale bars in both (a) and (b) represent 100 nm.

Drug Loading and *In Vitro* Release

IND is a kind of hydrophobic drug and is used to cure arthritic symptoms. Because of its small solubility in water, IND was used as hydrophobic drug model to study the drug load of the micelles. With increasing GP, the LC of the drug from the derivative micelles significantly increased. When GP increased from 92.49 to 131.72%, the LC of the drug increased from 19.32 to 31.37%. This indicated that with increasing GP, the number of PLA moieties in the core of the micelles increased; the intermolecular hydrophobic interactions between IND and PLA increased significantly, so the IND numbers penetrating into the core of micelles increased. Because of the increase of drug molecules loaded into micelles, the LE was higher from micelles of amphiphilic CS derivatives with higher GPs as the same quality of drug was added.

Figure 7(a) shows the release profiles of IND from the micelles in phosphate buffered saline (PBS). As shown in the figure, the release profile was divided into three stages: (1) burst release stage with 25–40% of the drug released in 5 h (the initial burst was possibly due to the drug deposited on the surface of the micelles), (2) slow-release stage with 10–15% of the drug released in 7 h (the drug in this stage was mainly released from the interior of the micelles at a low speed), and (3) equilibrium stage with gentle release. In this stage, the drug concentration varied little and basically reached equilibrium state. By comparing the drug-release profiles of CS–PLA with three different GPs, we observed that as GP increased from 92.49 to 131.72%, the cumulative release amount of the drug-loaded micelles decreased from 51.8 to 36.5% within 36 h, and the time required for the drug release to reach a balance increased from 8 to 10 h. With increasing PLA moieties, the intermolecular hydrophobic interaction increased, and the macromolecular chains combined closer as well; then, the binding ability of the micelles with hydrophobic IND increased accordingly. Thereby, the drugs were less prone to diffusion outside of micelles, and a slower release process was observed.

The release profiles of IND from the micelles formed by CS–PLA_{2a} in different pH solutions in PBS at 37°C (physiological environment) were studied. As shown in Figure 7(b), the release profile of drug release was also divided into three stages: (1) a burst release stage with 10–28% of the drug released in 5–10 h, (2) a slow-release stage with 20–30% of the drug released in 7 h, and (3) an equilibrium stage with gentle release. In certain range of pHs (6.1–8.0), the smaller pH was, the slower the drug release was. This was because in an acid environment, hydrogen bonds formed between the free aminos (—NH) in CS were

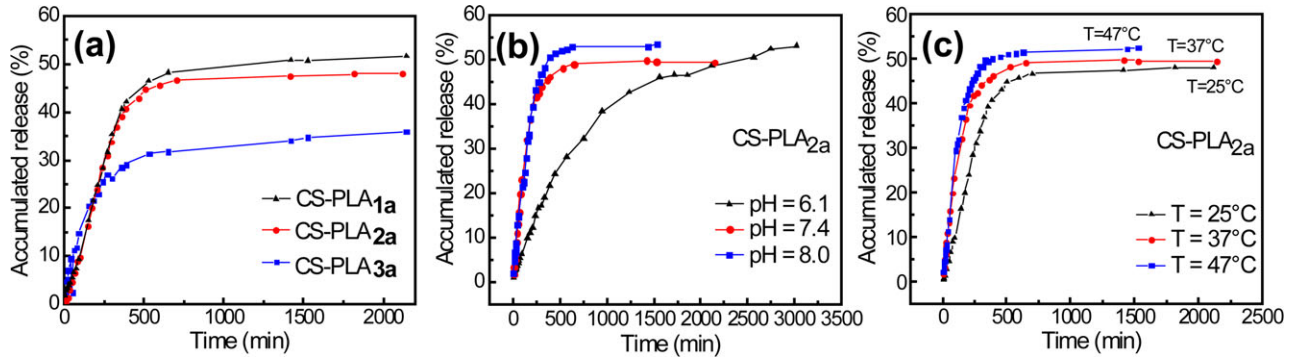

Figure 7. (a) Accumulated release profiles of IND from the micelles formed by amphiphilic CS derivatives in PBS [pH = 7.4, temperature (T) = 25°C]. (b) pH- and (c) temperature-dependent accumulated release profiles of IND from the CS–PLA_{2a} micelles. [Color figure can be viewed in the online issue, which is available at wileyonlinelibrary.com.]

Table III. Results of Indomethacin Release from the CS–PLA Nanoparticles with Different Grafting Efficiencies, pH Values, and Temperatures Fitted with Three Different Models

	First-order model				Weibull model			Higuchi model	
Sample	R^2	Q_∞	M	$K_1 \times 10^3$	R^2	b	$k \times 10^4$	R^2	K_H
CS-PLA_{1a}	0.986	51.6	53.3	3.6	0.892	0.556	5	0.839	1.48
CS-PLA_{2a}	0.986	48.0	51.8	4.2	0.853	0.517	4	0.772	1.46
CS-PLA_{3a}	0.977	36.0	33.8	4.5	0.885	0.388	1	0.707	1.10

	First-order model				Weibull model			Higuchi model	
pH (CS-PLA_{2a})	R^2	Q_∞	M	$K_1 \times 10^3$	R^2	b	$k \times 10^4$	R^2	K_H
6.1	0.999	53.0	51.9	1.2	0.979	0.655	5	0.973	1.05
7.4	0.986	48.0	51.8	4.2	0.853	0.517	4	0.772	1.46
8.0	0.993	54.8	54.3	5.7	0.742	0.826	4	0.747	2.03

	First-order model				Weibull model			Higuchi model	
Temperature (°C; CS-PLA_{2a})	R^2	Q_∞	M	$K_1 \times 10^3$	R^2	b	$k \times 10^4$	R^2	K_H
25	0.986	48.0	51.8	4.2	0.853	0.517	4	0.772	1.46
37	0.999	49.4	50.1	7.2	0.847	0.414	5	0.593	1.66
47	0.997	52.6	54. 8	8.3	0.848	0.455	9	0.593	2.20

much stronger; this made the diffusion of IND difficult. Notably, this could also be illustrated by the pH effect on the grain size of micelles determined by DLS.

Figure 7(c) shows the release profiles of IND from the micelles formed by CS–PLA_{2a} at different temperatures at pH 7.4. As shown in the figure, the typical three-stage release profile, including the burst release stage, slow-release stage, and equilibrium stage, were also observed. At 25–47°C, the drug release was fast: 250, 300, and 500 min were needed to reach the equilibrium stage at 47, 37, and 25°C, respectively. The accelerated drug-release process at higher temperatures may have been due to (1) the IND molecules diffusing faster as the temperature increased, (2) the decrease in the micellar volume caused by the partial dehydration of the PEG block, or (3) the accelerated degradation rate due to the higher hydrolysis rate at higher temperatures.[26,27]

With the development of drug-release systems, numerous mathematical models have also been developed for describing *in vitro* drug-release behaviors. In this study, the following frequently used zero-order kinetic model, first-order kinetic model, Weibull model, and Higuchi model were used to simulate the *in vitro* drug-release profile of the amphiphilic CS derivatives loaded with IND:[28,29]

1. Zero-order kinetic model:

$$Q_1 = Q_0 + K_0 t \tag{4}$$

where Q_1 is the accumulative percentage of the drug in the solvent when the time is t, K_0 is the constant of zero-order release, Q_0 is the initial concentration of the drug in the solvent, Q_0 is 0 in most cases, and t refers to the release time.

2. First-order kinetic model:

$$Q_1 = Q_\infty[1 - (M/Q_\infty)e^{-K_1 t}] \tag{5}$$

where K_1 refers to the constant of first-order release, Q_∞ is the largest accumulative release rate, and M is a constant.

3. Weibull model:

$$Q_1 = 1 - \exp\left[\frac{-(t - T_i)^b}{a}\right] \tag{6}$$

where a (>0) is shape parameter, b (>0) is scale parameter, and T_i is the location function. When $T_i = 0$, the formula is a two-parameter Weibull distribution.

4. Higuchi model:

$$Q_1 = K_H t^{1/2} \tag{7}$$

where K_H is the Higuchi diffusion constant, t is the time (minute).

Table III shows the simulation parameters of the drug-release profile with the previous three drug release models. The first-order kinetic model was closer to the experimental data than the other two models. The correlation coefficients (R^2's) of the three models were all larger than 0.97; this indicated that the *in vitro* drug-release pattern of the drug-loaded micelles of the amphiphilic CS derivatives in IND were basically in accordance with the model. Therefore, the *in vitro* drug release of the CS–PLA drug-loaded micelles could be best described with the first-order kinetic model; thus, the first-order model could be used to predict drug release and provide guidance for the clinical application of this drug.

CONCLUSIONS

In this study, amphiphilic CS derivatives containing side chains of PLA were successfully synthesized *in situ* through ring-opening graft polymerization with stannous octoate as the catalyst.

With a fixed stannous octoate content of 0.10%, a reaction temperature of 120°C, and a reaction time of 5 h, when the mass ratio of lactic acid to CS increased from 10 : 1 to 50 : 1, GP increased from 92.49 to 167.32%. With a fixed mass ratio of lactic acid to CS of 30 : 1, a reaction temperature of 120°C, and a reaction time of 5 h, when the catalyst content increased from 0.10 to 0.30%, GP increased from 131.72 to 313.42%. With a fluorescence probe method, DLS, and TEM, we found that the derivatives formed micelles in a water solution, with a grain size distributed from 169.8 to 260.7 nm and CACs from 0.048 to 0.021 mg/mL. With IND as the hydrophobic model drug, the drug load and release pattern of the derivatives micelles were also studied, and we found that when GP increased from 92.49 to 131.72%, the corresponding embedding rate of the drug increased from 19.31 to 31.37%, the accumulative release amount of the drug-loaded micelles within 36 h decreased from 51.8 to 36.5%, and the time required for the drug release to reach a balance increased from 8 to 10 h. The drug-release behaviors could be best described with a first-order kinetic model. These results suggest that CS–PLA may be used as a new drug-delivery vector for future clinical applications.

ACKNOWLEDGMENTS

This study was supported by the National Natural Science Foundation of China (contract grant number 21104068), Educational Commission of ZheJiang Province of China (contract grant number Y201121238), Zhejiang Province Public Welfare Project (contract grant number 2012C23098), the faculty seed fund of Hangzhou Dianzi University Foundation for Natural Sciences (contract grant number KYS225609011), and the Priority Academic Program Development of Jiangsu Higher Education Institutions.

REFERENCES

1. Qian, L.; Zhang, H. F. *Green Chem.* **2010**, *12*, 1207.
2. Thanou, M.; Verhoef, J. C.; Junginger, H. E. *Adv. Drug Delivery Rev.* **2001**, *50*, 91.
3. Sinha, V. R.; Singla, A. K.; Wadhawan, S.; Kaushik, R.; Kumria, R.; Bansal, K.; Dhawan, S. *Int. J. Pharm.* **2004**, *274*, 1.
4. Borchard, C. *Adv. Drug Delivery Rev.* **2001**, *52*, 145.
5. Khor, E.; Lim, L. Y. *Biomaterials* **2003**, *24*, 2339.
6. Kuritu, K. *Marine Biotechnol.* **2006**, *8*, 203.
7. Hudson, S. M.; Smith, C. In Biopolymers from Renewable Resources; Kaplan, D. L., Ed. Springer: Berlin, **1998**.
8. Kurita, K. *Prog. Polym. Sci.* **2001**, *26*, 1921.
9. Xie, H. B.; Zhang, S. B.; Li, S. H. *Green Chem.* **2006**, *8*, 630.
10. Okuda, T.; Ishimoto, K.; Ohara, H.; Kobayashi, S. *Macromolecules* **2012**, *45*, 4166.
11. Castillo, J. A.; Borchmann, D. E.; Cheng, A. Y.; Wang, Y. F.; Hu, C. H.; Garcia, A. J.; Weck, M. *Macromolecules* **2012**, *45*, 62.
12. Wasewar, K. L.; Yawalkar, A. A.; Moulijn, J. A.; Pangarkar, V. G. *Ind. Eng. Chem. Res.* **2004**, *43*, 5969.
13. Lu, H. W.; Zhang, L. M.; Wang, C.; Chen, R. F. *Carbohydr. Polym.* **2011**, *83*, 1499.
14. Teramoto, Y. S.; Nishio, Y. S. *Polymer* **2003**, *44*, 2701.
15. Chen, L.; Ni, Y. S.; Bian, X. C.; Qiu, X. Y.; Zhuang, X. L.; Chen, X. S.; Jing, X. B. *Carbohydr. Polym.* **2005**, *60*, 103.
16. Amass, W.; Amass, A.; Tihge, B. *Polym. Int.* **1998**, *47*, 89.
17. Jiang, G. B.; Quan, D. P.; Liao, K. R.; Wang, H. H. *Mol. Pharm.* **2006**, *3*, 152.
18. Feng, H.; Dong, C. M. *Biomacromolecules* **2006**, *7*, 3069.
19. Zhang, C.; Ping, Q.; Zhang, H. G.; Shen, J. *Eur. Polym. J.* **2003**, *39*, 1629.
20. Amiji, M. M. *Carbohydr. Polym.* **1995**, *26*, 211.
21. Whihelm, M.; Zhao, C. L.; Wang, Y.; Xu, R. L; Winnik, M. A.; Mura, J. L.; Riess, G.; Croucher, M. D. *Macromolecules* **1991**, *24*, 1033.
22. Liu, C. G.; Kashappa, G. D.; Chen, X. G.; Park, H. J. *J. Agric. Food Chem.* **2005**, *53*, 437.
23. Lee, K. Y.; Jo, W. H.; Kwon, I. C.; Kim, Y. H.; Jeong, S. Y. *Langmuir* **1998**, *14*, 2329.
24. Feng, H.; Dong, C. M. *Biomacromolecules* **2006**, *7*, 3069.
25. Gao, H.; Wang, Y. N.; Fan, Y. G.; et al. *J. Controlled Release* **2005**, *107*: 158.
26. Li, Y.; Rodrigues, J.; Tomás, H. *Chem. Soc. Rev.* **2012**, *41*, 2193.
27. He, C.; Kim, S. W.; Lee, D. S. J. *Controlled Release* **2008**, *127*, 189.
28. Costa, P.; Manuel, J.; Lobo, S. *Eur. J. Pharm. Sci.* **2001**, *13*, 123.
29. Lu, D. K.; Mao, A. I. *Int. J. Pharm.* **1996**, *129*, 243.